Available online at www.sciencedirect.com
SCIENCE DIRECT
Journal of Photochemistry and Photobiology A: Chemistry 179 (2006) 339–347
Journal of Photochemistry and Photobiology A:Chemistry
www.elsevier.com/locate/jphotochem

Probing of photocatalytic surface sites on SO_4^{2-}/TiO_2 solid acids by in situ FT-IR spectroscopy and pyridine adsorption

Xinchen Wang [a], Jimmy C. Yu [b], Ping Liu [a], Xuxu Wang [a], Wenyue Su [a], Xianzhi Fu [a,*]

[a] *Research Institute of Photocatalysis, Chemistry and Chemical Engineering College, Fuzhou University, Fuzhou, Fujian 350002, China*
[b] *Department of Chemistry and Environmental Science Program, The Chinese University of Hong Kong, Shatin, New Territories, Hong Kong, China*

Received 17 May 2005; received in revised form 1 August 2005; accepted 6 September 2005
Available online 11 October 2005

Abstract

Photocatalytic surface sites on SO_4^{2-}/TiO_2 were investigated by pyridine adsorption and in situ Fourier transform infrared (FT-IR) spectroscopy. Results revealed that the sulfate-modification not only increased the number of strong Lewis acidic sites, but also induced a large amount of strong Brønsted acidic sites on the surface of TiO_2. Pyridine molecules were chemically captured on Brønsted and Lewis acidic sites on the SO_4^{2-}/TiO_2 surface. These pyridine molecules were progressively decomposed to final products of CO_2 and H_2O under actual photocatalytic conditions. The high photocatalytic performance of SO_4^{2-}/TiO_2 can be explained by the improved surface acidities that favor the adsorption of both oxygen and pyridine molecules. Moreover, the Lewis acidic sites could react with H_2O and was then converted to Brønsted acidic sites, leading to the activation of the water. This conversion promoted the formation of hydroxyl groups on the catalyst surface, which could also contribute to the high photocatalytic reactivity of SO_4^{2-}/TiO_2.

Keywords: Photocatalyst; Surface acidity; Hydroxyl groups; FT-IR; Superacids; Titania; In situ

1. Introduction

Photochemical reactions on the surface of light-activated semiconductors (e.g. TiO_2) are attracting considerable academic and industrial interest because of their promising applications in solar cells, water splitting, and environmental purification [1]. The efficiencies of these photo-assisted reactions are strongly dependent on the crystal phase, size, and pore-wall structure as well as the surface chemistry, particularly surface acidity, of the TiO_2 photocatalyst [2]. This knowledge, together with novel approach to material synthesis, is contributing to the design and development of new TiO_2-based photocatalysts with high activity and stability for commercial applications such as air purification.

Solid acids are green catalysts widely used in a number of industrially important reactions including isomerizations, alkylations, catalytic reforming of alkanes, and cracking [3]. Recently, TiO_2-based solid acids have been introduced into the photocatalysis field as efficient photocatalysts for the elimination of volatile organic compounds (VOCs) in air [4]. It was found that the solid acid photocatalysts possessed higher activity than pure TiO_2 for the photocatalytic oxidation (PCO) of CH_3Br, C_2H_4, and C_6H_6. For example, the photocatalytic conversion of CH_3Br over SO_4^{2-}/TiO_2 was six times higher than that over TiO_2. Moreover, $SO_4^{2-}/TiO_2$was much more stable than pure TiO_2; after PCO for 6 h, SO_4^{2-}/TiO_2 was not deactivated, whereas for TiO_2 the conversion decreased from 88 to 29% for C_6H_6 and from 60 to 12% for CH_3Br [4]. These improvements have previously been attributed to high specific surface area and large fraction of anatase–TiO_2 on SO_4^{2-}/TiO_2 [4]. However, this explanation based simply on bulk characterizations is inadequate as the reactivity of a photocatalyst is also strongly dependent on its surface properties. Therefore, it is of significant interest from a fundamental viewpoint to study the surface photochemical processes, particularly the role of surface acidities, on SO_4^{2-}/TiO_2 at the molecular level, which, to the best of our knowledge, is not yet available.

It is known that surface acidities play an important role on photocatalytic processes. One of the cost-effective ways to improve the photocatalyst performance is to increase the number

* Corresponding author. Fax: +86 591 83738608.
E-mail address: xzfu@fzu.edu.cn (X. Fu).

1010-6030/$ – see front matter © 2005 Elsevier B.V. All rights reserved.
doi:10.1016/j.jphotochem.2005.09.007

and the strength of surface acidic sites because the photocatalytic activity has been shown to increase with photocatalyst surface acidity. For example, doping TiO_2 with metal oxides such as Nb_2O_5 [5a], WO_3 [5b], MoO_3 [5b], ZrO_2 [5c], and SiO_2 [5c] was reported to increase the surface acidity and photocatalytic activity of TiO_2. The sulfated metal oxides are strong acids that are classified as solid superacids. Sulfated TiO_2 can be readily synthesized by the reaction of amorphous TiO_2 with a source of sulfur compounds (e.g. H_2SO_4, $(NH_4)_2SO_4$, SO_2) at high temperatures. The solid acids are recently employed as photocatalysts [4,5d]. Indeed, little work has been done to study the photocatalytic properties of SO_4^{2-}/TiO_2, especially the probing of nature of surface acidic structure under real photocatalytic conditions.

In situ characterization of surface species and surface active sites during heterogeneous catalytic/photocatalytic processes is one of the most important approaches to investigate a reaction mechanism. A number of spectroscopic techniques (e.g. NMR [6], ESR [7], and FT-IR [8]) or thermally programmed methods [9] have been employed to study directly photocatalytic reactions on the surface of TiO_2. Among these, FT-IR is probably the best method for in situ photocatalytic studies because it is inexpensive, sensitive, of good resolution, and capable of determining chemical species [10]. Most notably, FT-IR measurements can be carried out at atmospheric pressure and room temperature. These ambient conditions are identical to those in which the photocatalytic reactions usually take place. The in situ FT-IR technique has been used in studying the photocatalytic decomposition of acetic acid [8c], glyoxylic acid [8b], dichloromethane [6d], ethanol [8d,e], and acetone [8d]. However, the methods reported in the literature tell us very little about the nature of photocatalytic active sites.

The nature of the surface active sites in solid acids is defined by the presence of protons, generating Brønsted acidic sites, and by co-ordinately unsaturated cationic centers giving Lewis acidity [3]. The adsorption of base molecules (e.g. pyridine or ammonia) combined with vibrational spectroscopic techniques, is well known for characterizing these surface active sites [10c,d]. The narrow-band widths of pyridine adsorbed on acidic sites make this a particular favorite for infrared spectroscopic studies, giving good resolution of ring vibrational modes to distinguish between Brønsted ($\sim$1540 cm^{-1}) and Lewis ($\sim$1450 cm^{-1}) adsorbed forms [3]. Moreover, pyridine is a commonly found hazardous substance with stable aromatic structure [11]. The choice of this representative organic pollutant as a molecular probe for studying photocatalytic surface chemistry is desirable.

In the current paper we report an in situ FT-IR method for investigating photocatalytic surface sites on SO_4^{2-}/TiO_2 solid acids using pyridine as a target molecule. Pyridine serves two functions, namely (1) as a model volatile organic pollutant and (2) as a molecular probe for determining surface structure and reaction mechanism of the solid acid photocatalysts. The findings in this study help in explaining the high activity and stability of the SO_4^{2-}/TiO_2 photocatalyst toward the decomposition of VOCs.

2. Experimental

2.1. Catalyst preparation

The SO_4^{2-}/TiO_2 solid acids were synthesized by reacting amorphous TiO_2 with H_2SO_4 at high temperatures. The amorphous TiO_2 xerogel was firstly prepared by a sol–gel method [12]. This TiO_2 xerogel was then submerged in a 1 M H_2SO_4 solution (1 g TiO_2:1 mL H_2SO_4). The mixture was sonicated under reduced pressure for 2 min. This effectively removed the air trapped in the porous TiO_2 and drove the H_2SO_4 into the pore networks, leading to a homogeneous adsorption of SO_4^{2-} on the surface of TiO_2 [13]. After that, the mixture was dried at 80 °C for 24 h to remove water. The resulting solids were sintered at 450 °C for 3 h to obtain the SO_4^{2-}/TiO_2 solid acids. For comparison, pure TiO_2 was also prepared by sintering the amorphous TiO_2 at 300 °C. In terms of the Hammett acidity parameter, H_0, the acid strength of SO_4^{2-}/TiO_2 was found to be more negative than −12.44. This was much stronger than pure TiO_2 ($H_0 > -3.0$).

2.2. Characterization

X-ray photoelectron spectroscopy (XPS) measurements were carried out by using a VG Scientific ESCA Lab Mark II spectrometer equipped with two ultra-high vacuum (UHV) chambers. All binding energies were referenced to the C_{1s} peak at 284.8 eV of the surface adventitious carbon. IR spectra on KBr pellets of the samples were recorded on a Nicolet 410 FT-IR spectrometer at a resolution of 4 cm^{-1}. The concentration of sample in KBr was kept around 0.3%. The nitrogen adsorption–desorption isotherms at 77 K were measured using a Micrometerics ASAP2010 system after the samples were vacuum-dried at 180 °C overnight. X-ray diffraction (XRD) measurements were performed on a Bruker D8 Advance X-ray diffractometer with Cu Kα radiation. The crystal size was calculated from the full width at half maximum (fwhm) of anatase (1 0 1) using Sherrer equation. Temperature programmed desorption (TPD) of oxygen molecules was carried out by using a Micrometerics TPD/R2910 chemisorbed instrument. Sample (0.4 g) was pre-treated at 150 °C under Ar gas for 1 h. The sample was then cooled down to room temperature. Continuous pluses of oxygen were subsequently injected over the catalyst until the sample reached the adsorption equilibrium. After this, the sample was heated from 30 to 600 °C at a rate of 10 °C min^{-1} using Ar as carrier gas (flow rate: 10 mL min^{-1}). The desorption of oxygen molecules was monitored by a thermal conductivity detector. The amount of adsorbed oxygen was calculated according to the area of O_2-desorption peaks.

2.3. Photocatalytic activity

The measurement of photocatalytic activity was carried out in a fixed bed tubular quartz reactor operated in a single-pass mode. The reactor was surrounded with four 8 W UV bulbs (365 nm). The weight of the catalyst was kept constant at 0.25 g. Bromomethane diluted with zero air was used to afford a reac-

tant stream. The initial concentrations of CH_3Br and CO_2 in the stream were 300 and 0 ppm, respectively. The flow rate of reactant stream was kept at 20 mL min^{-1}. Analysis of the reactor effluent was conducted with a gas chromatograph (Hewlett-Packard 6890) equipped with a flame ionization detector, a thermal conductivity detector, and a Porapak R column. As a comparison, the photocatalytic activity of commercial Degussa P25, a reference titania catalyst, was also tested.

2.4. In situ FT-IR study

In situ investigation of photocatalytic surface reactions on SO_4^{2-}/TiO_2 was performed on a Nicolet 410 FT-IR spectrometer. The experiments were carried out in a special IR cell (supporting materials, Fig. S1). The UV-transparent quartz cell contained two CaF_2 windows that were transparent in the IR region. Inside the cell, there was a rotational sample holder that was attached to a heater and a K-type thermocouple. These devices, in conjunction with a water-cooling system and a vacuum system, provided accurate temperature control (±1 K) and high vacuum (<l × l0^{-4} Torr). The detailed experimental procedures were as follows. The sample (ca.12 mg/cm^{-2}) was pressed into a self-supporting thin wafer and then put into the sample holder. The wafer was degassed in dynamic vacuum (1 × l0^{-4} Torr) at 393 K for 3 h, and then the background spectra were recorded. After equilibration of adsorption of pyridine vapor for 15 min, the spectra were recorded after degassing the wafer under vacuum at 393 K and l × l0^{-4} Torr for 1 h. In order for the in situ FT-IR observation of photocatalytic reaction on SO_4^{2-}/TiO_2 under actual photocatalytic conditions, the air and UV light were then introduced into the cell loaded with pyridine-adsorbed wafer to begin the experiments. The UV illumination of the wafer was provided by an 8 W 365 nm UV bulb. The incident intensity of UV light at the position of the wafer surface was approximately 2 mW/cm^2. Since the background carbon dioxide level in the atmosphere was too high, it was difficult to detect the CO_2 evolved from the photo-oxidation of pyridine given the tiny amount of catalyst (∼12 mg) involved. In order to solve this problem, a 10 cm long 2.4 mm diameter tube-like quartz reactor loaded with 2 g catalyst was specially designed for detecting CO_2 produced from the reaction. The tube-like quartz reactor was coupled to the gas chromatograph for analyzing CO_2.

3. Results and discussion

3.1. Rule out the effect of bulk properties

It was noted that both bulk properties (e.g. surface area, crystal phase, and crystal size) and surface properties considerably affect the photocatalytic activity of TiO_2. In our previous studies [4], we only compared the photocatalytic activities of sulfated TiO_2 and pure TiO_2 with a calcination temperature of 450 °C. At this temperature, SO_4^{2-}/TiO_2 possesses larger specific surface area and higher surface acidity than pure TiO_2. So, the improved photocatalytic performance of SO_4^{2-}/TiO_2 might be attributed to the increased specific surface area. In order to exclude the effect of surface area, in this study, the sol–gel-derived pure

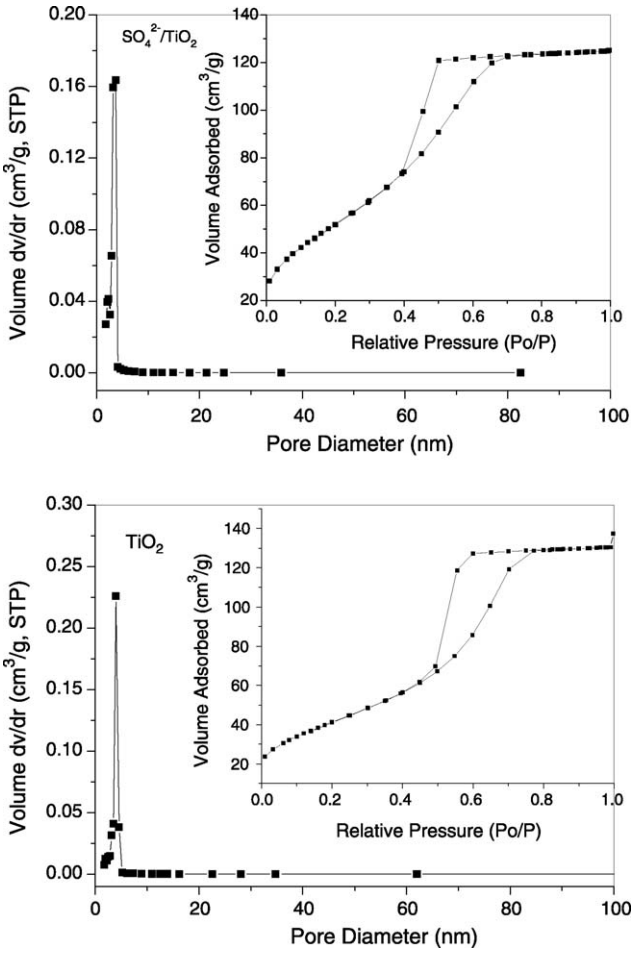

Fig. 1. N_2-sorption isotherms (inset) and corresponding BJH pore size distribution curves for the TiO_2 and SO_4^{2-}/TiO_2 samples.

TiO_2 was calcined at 300 °C whereas sulfated TiO_2 at 450 °C. As a result, the two samples possessed similar specific surface area and crystal size. As shown in Figs. 1 and 2 and Table 1, both specific surface area (∼150 m^2 g^{-1}) and anatase crystal size

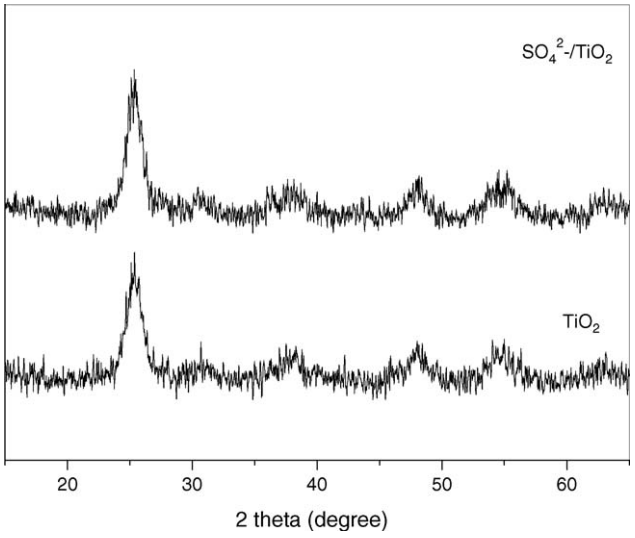

Fig. 2. X-ray diffraction (XRD) patterns of pure TiO_2 and SO_4^{2-}/TiO_2 samples.

Table 1
Physical and chemical properties of the SO_4^{2-}/TiO_2 and synthesized TiO_2 photocatalysts

Sample	S_{BET} ($m^2\ g^{-1}$)[a]	V^b ($cm^3\ g^{-1}$)[b]	D_{BJH} (nm)[c]	Crystal phase	Crystal size (nm)[d]	Adsorbed oxygen (mmol g^{-1})[e]
SO_4^{2-}/TiO_2	153	0.21	4.4	Anatase	5.6	0.54
TiO_2	152	0.22	4.6	Anatase	5.3	0.31

[a] BET surface area calculated from the linear part of the BET plot ($P/P_0 = 0.1$–0.2).
[b] Total pore volume, taken from the volume of N_2 adsorbed at $P/P_0 = 0.995$.
[c] Average pore diameter, estimated using the desorption branch of the isotherm and the Barrett–Joyner–Halenda (BJH) formula.
[d] Average crystal size of anatase–TiO_2, estimated using Scherrer equation.
[e] The amount of adsorbed oxygen was obtained from O_2-TPD results.

(~6 nm) for SO_4^{2-}/TiO_2 and pure TiO_2 were virtually identical. The photocatalytic activity of SO_4^{2-}/TiO_2, pure TiO_2 and reference titania (Degussa P25) was shown in Fig. 3. The SO_4^{2-}/TiO_2 showed higher photocatalytic conversion of CH_3Br (55%) than that of pure TiO_2 (12%) and Degussa P25 (11%). The concentration of produced CO_2 (164 ppm) from SO_4^{2-}/TiO_2 was also higher than those from pure TiO_2 (66 ppm) and P25 (60 ppm). In addition, the SO_4^{2-}/TiO_2 sample was stable during the whole reaction, while serious deactivation was observed for both pure TiO_2 and Degussa P25. Obviously, the enhanced photocatalytic performance of SO_4^{2-}/TiO_2 in our study was mainly due to the changes of surface properties by sulfate-modification of TiO_2.

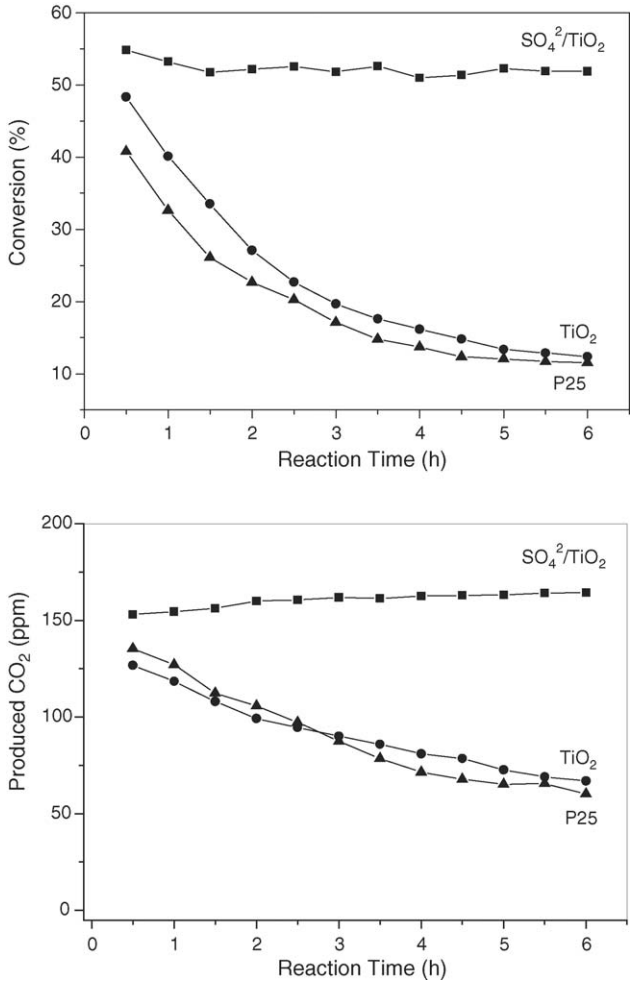

Fig. 3. Photocatalytic conversion of CH_3Br over pure TiO_2 and SO_4^{2-}/TiO_2. As a comparison, the photocatalytic activity of Degussa P25 titania was also tested.

3.2. Surface sulfur species

The structure of sulfur complexes on the surface of TiO_2 was examined by XPS and IR measurements. Fig. 4a showed the XPS spectrum in the S_{2p} binding energy (BE) region for

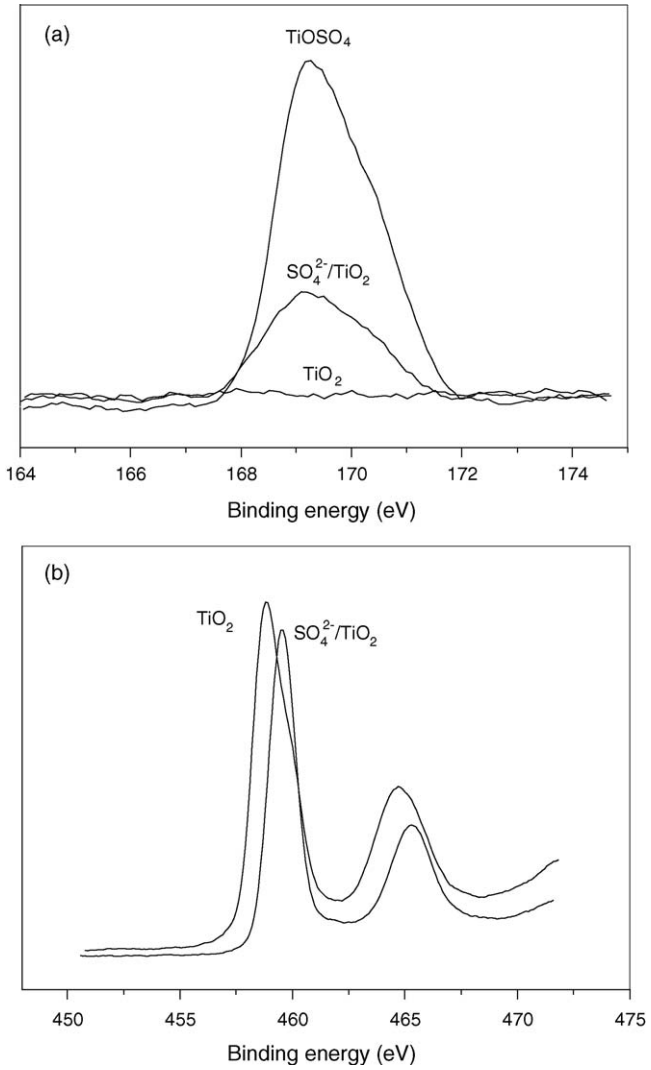

Fig. 4. XPS spectra of TiO_2, SO_4^{2-}/TiO_2 and $TiOSO_4$ samples in (a) S_{2p} and (b) Ti_{2p} binding energy regions.

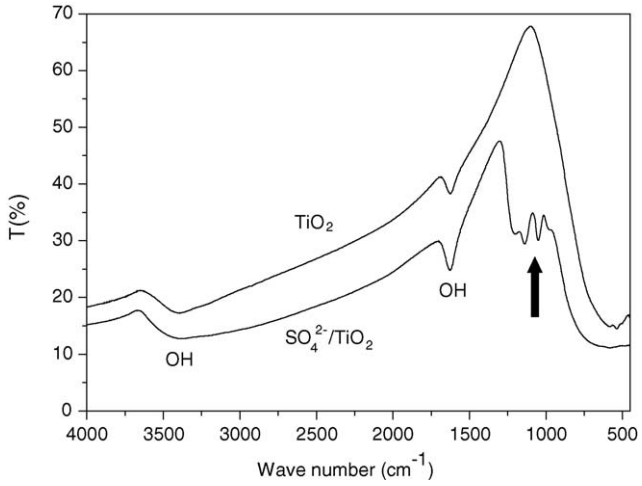

Fig. 5. Infrared spectra of pure TiO_2 and SO_4^{2-}/TiO_2 catalysts. The broad peak at ~3400 cm^{-1} corresponds to the O–H stretch region [30], whereas the peak at ~1630 cm^{-1} results from the O–H bending of adsorbed water molecules [31].

TiO_2, SO_4^{2-}/TiO_2, and $TiOSO_4$. There was no sulfur signal on pure TiO_2, whereas for the SO_4^{2-}/TiO_2 catalyst the BE of $S_{2p3/2}$ was observed at 168.4 eV. The BE of 168.4 eV suggested that the sulfur in SO_4^{2-}/TiO_2 existed in a six-oxidation state (S^{6+}) [14]. This was confirmed by the XPS measurement of $TiOSO_4$, in which the sulfur exists typically in the form of S^{6+} and possesses a BE of 168.4 eV (Fig. 4a). Fig. 5 showed the IR spectra of SO_4^{2-}/TiO_2 and pure TiO_2. Several absorption peaks in the 900–1300 cm^{-1} region were observed on the spectra for SO_4^{2-}/TiO_2 but absent on the one for the pure TiO_2. The peaks at 1219, 1135, 1048, and 976 cm^{-1} were the characteristic frequencies of a bidentate SO_4^{2-} co-ordinated to metals such as Ti^{4+} (Scheme 1) [14a,15]. It was noted that such a bridge bidentate structure could strongly withdraw electrons from the neighboring Ti cations, resulting in an up-shifting of BE of the Ti cations. As shown in Fig. 4b, $Ti_{2p3/2}$ BE of 458.8 eV was observed for pure TiO_2, while the $Ti_{2p3/2}$ BE of the SO_4^{2-}/TiO_2 sample shifted to a higher value of 459.9 eV, indicating a very strong interaction between the sulfate anion and titanium cation. Such an interaction has also been reported by Anderson and co-workers [12], and is believed to be a driving force in the generation of a large amount of surface acidic sites on solid acids of sulfated metal oxides [16].

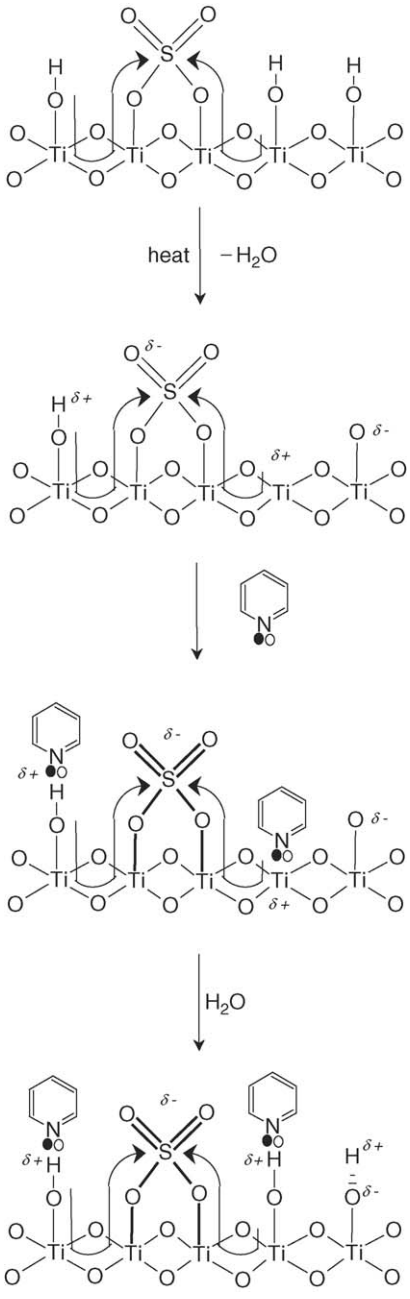

Scheme 1. Probing of surface active sites on the SO_4^{2-}/TiO_2 solid acid using pyridine as an adsorption molecule.

3.3. Adsorption of pyridine vapor on SO_4^{2-}/TiO_2

Before photocatalytic reaction, in order to obtain a relatively clean surface, the SO_4^{2-}/TiO_2 catalyst was pre-treated at 393 K under vacuum for 3 h. Pyridine was then adsorbed onto the surface of SO_4^{2-}/TiO_2. The sample was subsequently degassed at 393 K for 1 h to remove physically adsorbed pyridine. The chemisorptive states of the pyridine molecules were examined by FT-IR. As shown in Fig. 6b, the spectrum contained several significant peaks at 1445, 1489, 1540, 1607 and 1639 cm^{-1}. These peaks could be assigned to the chemisorption of molecular pyridine at different type of surface acidic sites [17]. The peaks at 1445 and 1607 cm^{-1} were due to the interaction of pyridine with Lewis acidic sites (exposed Ti^{4+} cations), while the peaks at 1540 and 1639 cm^{-1} came from the protonation of pyridine molecule by the Brønsted acid sites (surface-bound hydroxyl groups) [17]. The peak at 1489 cm^{-1} was due to the vibration of pyridine adsorbed on Brønsted acidic sites and on Lewis acidic sites [17]. It should be noted that only small peaks corresponding to pyridine adsorbed on Lewis acidic sites were observed for pure TiO_2 (Fig. 6a). This suggested that the surface acidities of pure TiO_2 were too weak to react with pyridine molecules. Evidently, sulfate-modification not only increased the number of strong Lewis acidic sites, but also induced a large amount of strong Brønsted acidic sites on the surface of TiO_2 (Fig. 6b).

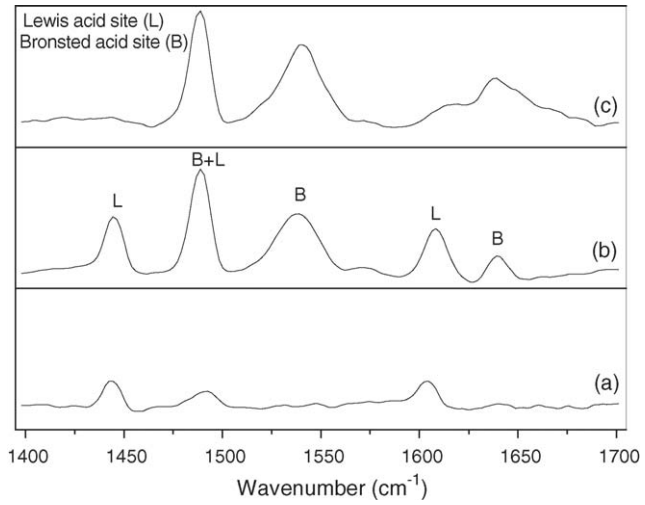

Fig. 6. Infrared spectra of pyridine molecules adsorbed on (a) TiO_2 and (b) SO_4^{2-}/TiO_2 catalysts under vacuum. The spectrum of (c) is corresponded to (b) upon contact with atmosphere (humidity 80%).

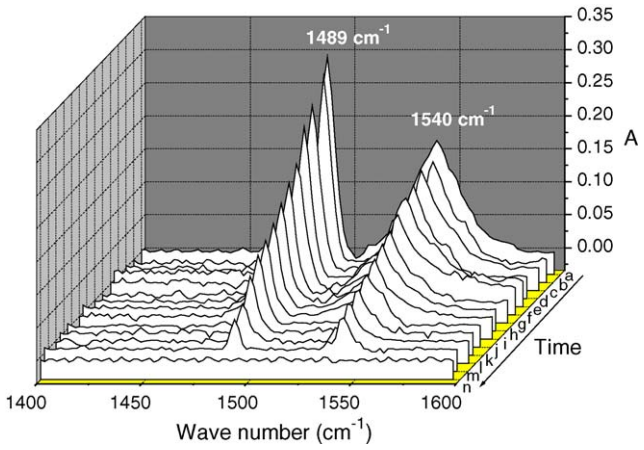

Fig. 7. Infrared spectra recorded during 365 nm UV illumination of pyridine on SO_4^{2-}/TiO_2 in actual photocatalytic conditions. Background spectrum was that of SO_4^{2-}/TiO_2 catalyst without adsorbing pyridine. Spectra were obtained from data collections initiated (a) 0 min, (b) 5 min, (c) 10 min, (d) 30 min, (e) 60 min, (f) 90 min, (g) 120 min, (h) 150 min, (i) 210 min, (j) 260 min, (k) 310 min, (l), 360 min, (m) 420 min, and (n) 600 min after irradiation began. Each spectrum was scanned 64 times with a resolution of 4 cm^{-1}.

These strong Brønsted and Lewis acidic sites may provide better adsorption centers for reactant molecules. Although the role of such surface acidities on acid-catalyzed reactions have been well studied in the field of conventional catalysis, the photochemical behaviors of these strong acidic sites during heterogeneous photocatalysis is still less reported.

3.4. Photocatalytic oxidation of the adsorbed pyridine

As photocatalytic reactions generally take place at ambient conditions, the pyridine-adsorbed SO_4^{2-}/TiO_2 was exposed to the atmosphere (80% humidity). Upon exposure to the atmosphere, the Lewis acidic sites reacted with H_2O molecules and were converted to Brønsted acidic sites (Fig. 6c). This conversion was proved by the disappearance of the peak at 1445 cm^{-1} and the enhancement in the peak area of pyridine adsorbed at the Brønsted acidic sites (1540 cm^{-1}) from original 3.184 to 4.629 after adsorption of water. As the Lewis acidic sites were converted to Brønsted acidic sites after reacting with H_2O, at this moment, the peak at 1489 cm^{-1} was ascribed to one of the vibration modes of pyridine adsorbed on Brønsted acidic sites [17]. Fig. 7 showed the evolution of the spectral changes of pyridine-adsorbed sample over 600 min UV-irradiation. A gradual degradation of pyridine was observed, as evident by the progressive decrease in the intensities of peaks at 1489 and 1540 cm^{-1} for the adsorbed pyridine. After reaction for 600 min, the peaks completely disappeared. This indicated that the pyridine molecules adsorbed on the Brønsted acidic sites were completely decomposed. Fig. 8 showed the evolution of CO_2 from the photocatalytic oxidation of pyridine. This further confirmed that the disappearance of the pyridine-adsorbed peaks upon UV-irradiation was due to the photocatalytic conversion of pyridine to final product CO_2, instead of photo-desorption of pyridine molecule from the Brønsted acidic sites. It was noted that when the TiO_2 sample was exposed to humid atmosphere, the pyridine absorption peak at 1445 cm^{-1} was almost completely disappeared without accompanying by the formation

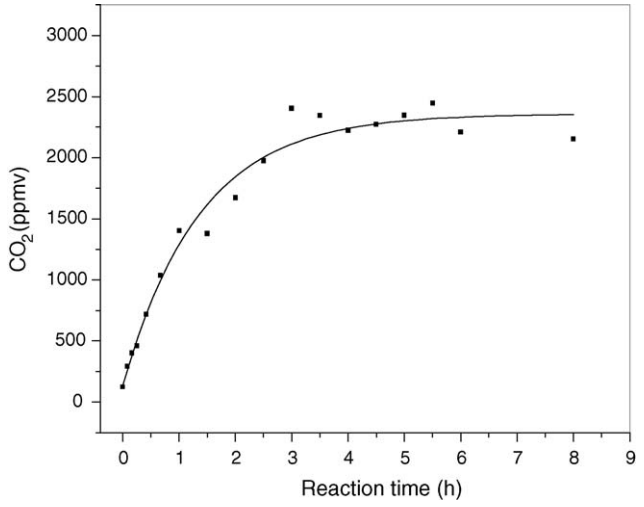

Fig. 8. The amount of carbon dioxide produced from the pyridine photodecomposition on the SO_4^{2-}/TiO_2 photocatalyst as function of reaction time.

of a new peak at 1540 cm^{-1}. This revealed that no Lewis-to-Brønsted acidic site conversion occurred on the pure TiO_2 sample. The disappearing of peak at 1445 cm^{-1} was due to the desorption of pyridine molecules from TiO_2 surface with weak acidity.

4. Discussion

Due to the strong electron-inducing effect of the surface sulfur complex, a large number of Brønsted and Lewis acidic sites were created on the surface TiO_2. These acidic sites could provide more surface chemisorption centers for reactants. The formation of chemisorbed species on the surface sites upon pyridine adsorption could be summarized in Scheme 1. When the pyridine-adsorbed sample was exposed to real photocatalytic atmosphere, the Lewis acidic sites were converted to Brønsted

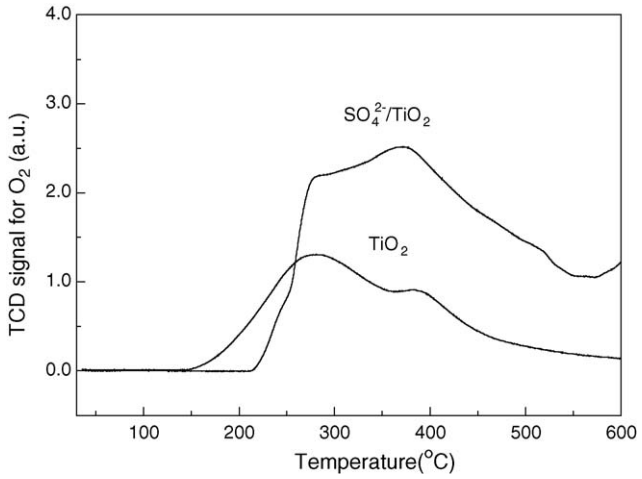

Fig. 9. TPD spectra for O_2 adsorbed on TiO_2 and SO_4^{2-}/TiO_2 samples.

acidic sites by the dissociation of water. The Brønsted acidic sites generally take the form of surface-bounded hydroxyl groups. It has been indicated by previous investigators that the surface hydroxyl groups play an important role in photocatalytic degradation of organic compounds [2e–g]. The high density of surface hydroxyl groups could improve the chemisorption capability of TiO_2 surfaces toward reactant molecules. In fact, our experimental results have also confirmed the improved chemisorption capability, as revealed by O_2-TPD measurements in Fig. 9 and Table 1. For the pure TiO_2, the adsorption amount of O_2 was 0.31 mmol g^{-1}, whereas for the SO_4^{2-}/TiO_2 it significantly increased to 0.54 mmol g^{-1}. It is commonly held that the adsorbed oxygen molecules are of vital importance for both liquid- and gas-phase heterogeneous photocatalysis. Among various primary photocatalytic processes on TiO_2, the interfacial transfer of photo-induced electron is the slowest step, and therefore, it is a rate-determining step [1d]. As the O_2 scavenge the photoexcited electrons from the conduction band of TiO_2, the increase in the oxygen adsorption is favorable for the interfacial transfer of photoexcited electrons. Although the importance of surface hydroxyl groups in adsorption on TiO_2 surfaces and in promoting interfacial transfer of electron has been discussed in the literature [1,18a,19], this is the first report that describes the similar results for the SO_4^{2-}/TiO_2 solid acid photocatalysts.

Moreover, the surface hydroxyl groups may also have significantly effect on the chemical behaviors of photoexcited holes. The reaction mechanism for photogenerated holes at the TiO_2 surfaces is a recent hot topic [20], and has not yet been definitively established [1e]. There generally exist two proposed reaction mechanisms for the photogenerated holes on TiO_2 photocatalyst: (1) the holes react with surface hydroxyl groups to produce highly active hydroxyl radials which initiate photooxidation reactions [1d,21]; (2) the holes are directly trapped by chemisorbed organic molecules [22–26]. Despite the disagreements on the reaction pathways of photogenerated holes, we believed that the high density of surface hydroxyl groups was helpful for both $^{\bullet}OH$-driven and direct hole oxidation pathways. In the $^{\bullet}OH$-driven pathway, the large amount of surface hydroxyl groups effectively trapped the holes, generating a large amount of reactive hydroxyl radicals [1d]; whereas in the case of direct hole oxidation mechanism, the high density of surface hydroxyl groups provided more surface sites for adsorbing organic molecules that also efficiently captured the photogenerated holes. This, together with the stabilization of photo-induced electrons by oxygen molecules, greatly prohibited the undesirable electron–hole pair recombination, improving the photocatalytic quantum efficiency.

Furthermore, H_2O was one of the final products in a photocatalytic reaction. This H_2O as well as water in atmosphere can easily adsorb onto the surface of TiO_2 due to the superhydrophilic nature of UV-excited TiO_2 surface [27]. The adsorbed water located in the outmost layer of TiO_2 surface would prevent the reactant molecules from adsorbing onto the inner active sites [28]. This was believed to be one of the main reasons that accounted for the gradual deactivation of TiO_2 during photocatalytic reactions [29]. However, for the sulfate-promoted TiO_2, the water molecule could be converted firstly to surface hydroxyl groups by dissociating on strong Lewis acidic sites. These hydroxyl groups subsequently captured photogenerated holes on SO_4^{2-}/TiO_2 and thereafter, producing highly reactive surface hydroxyl radicals. As a result, the water produced from photocatalytic reactions could be activated and enter into the reactions again. This might also contribute to the high catalytic performance of SO_4^{2-}/TiO_2 photocatalyst.

Additionally, the sulfated TiO_2 was known as a super-strong solid acid catalyst. Even in dark, the strong acidic sites were conceived to carry out catalytic reaction of a large number of organic compounds. Particularly, large and stable organics can easily be activated and cracked by superacid catalysts [3]. Meanwhile, the strong acidic sites might also attack the stable surface intermediates of photocatalytic reactions, inhibiting the buildup of surface species. The coupling of superacid catalysis with photocatalysis could remarkably change the pathways of photocatalytic reactions and facilitate the reactions that are difficult to take place on pure TiO_2. Study of this coupling effect is still in progress.

5. Conclusions

In situ FT-IR was shown to be useful in investigating photoinitiated surface reactions. This simple approach could precisely identify the surface species and the structure of active sites with the aid of a proper probing molecule. The sulfation of TiO_2 photocatalyst induced Brønsted acidic sites and increased Lewis acidic sites on the TiO_2 surface. The strong acidities imparted a high reactivity on TiO_2 surface toward adsorbing reactant and oxygen molecules. These, along with the stabilization of photogenerated charge carriers, led to the high photocatalytic efficiency. Moreover, deactivation caused by water adsorption could be avoided. This partly explained the high photocatalytic performance of SO_4^{2-}/TiO_2. Furthermore, the combination of superacid-catalyzed with photo-catalyzed processes was believed to alter the reaction routes, which might also favor the photodecomposition of organics, particularly stable aromatic compounds.

Acknowledgement

The work described here is financially supported by the National Natural Science Foundation of China (Nos. 20133010 and 20273014).

Appendix A. Supplementary data

Supplementary data associated with this article can be found, in the online version, at 10.1016/j.jphotochem.2005.09.007.

References

[1] (a) M. Grätzel, Nature 414 (2001) 338;
(b) A. Fujishima, K. Honda, Nature 37 (1972) 238;
(c) A. Mills, R.H. Davies, D. Worsley, Chem. Soc. Rev. (1993) 417;
(d) M.R. Hoffmann, S.T. Martin, W. Choi, D.W. Bahnemann, Chem. Rev. 95 (1995) 69;
(e) A.L. Linsebiler, G. Lu, J.T. Yates, Chem. Rev. 95 (1995) 735;
(f) P.V. Kamat, Chem. Rev. 93 (1993) 267;
(g) A. Hagfeldt, M. Gratzel, Chem. Rev. 95 (1995) 49;
(h) M.A. Fox, M.T. Dulay, Chem. Rev. 93 (1993) 341.

[2] (a) Z.B. Zhang, C.C. Wang, R. Zakaria, J.Y. Ying, J. Phys. Chem. B 102 (1998) 10871;
(b) C.C. Wang, Z. Zhang, J.Y. Ying, Nanostruct. Mater. 9 (1997) 583;
(c) X.Z. Fu, L.A. Clark, Q. Yang, M.A. Anderson, Environ. Sci. Technol. 30 (1996) 647;
(d) J.C. Yu, X.C. Wang, X.Z. Fu, Chem. Mater. 16 (2004) 1523;
(e) J. Papp, S. Soled, K. Dwight, A. Wold, Chem. Mater. 6 (1994) 496;
(f) Y.R. Do, W. Lee, K. Dwight, A.J. Wold, Solid State Chem. 108 (1994) 198;
(g) Y.H. Zhang, G.X. Xiong, N. Yao, W.S. Yang, X.Z. Fu, Catal. Today 68 (2001) 89;
(h) H. Cui, K. Dwight, S. Soled, A. Wold, Solid State Chem. 115 (1995) 187.

[3] A. Corma, Chem. Rev. 97 (1997) 2373 (and references therein).

[4] (a) X.Z. Fu, W.A. Zeltner, M.A. Anderson, Appl. Catal. B-Environ. 6 (1995) 209;
(b) X.Z. Fu, Z.X. Ding, W.Y. Su, Chin. J. Catal. 20 (1999) 321.

[5] (a) H. Cui, K. Dwight, S. Soled, A. Wold, Solid State Chem. 115 (1995) 187;
(b) J. Papp, S. Soled, K. Dwight, A. Wold, Chem. Mater. 6 (1994) 496;
(c) X.Z. Fu, L.A. Clark, Q. Yang, M.A. Anderson, Environ. Sci. Technol. 30 (1996) 647;
(d) D.S. Muggli, L.F. Ding, Appl. Catal. B-Environ. 32 (2001) 181.

[6] (a) S.J. Hwang, C. Petucci, D. Raftery, J. Am. Chem. Soc. 119 (1997) 7877;
(b) S.J. Hwang, C. Petucci, D. Raftery, J. Am. Chem. Soc. 120 (1998) 4388;
(c) A.Y. Nosaka, T. Fujiwara, H. Yagi, H. Akutsu, Y. Nosaka, Langmuir 19 (2003) 1935;
(d) J. Borisch, S. Pikenton, M.L. Miller, D. Raftery, J.S. Francisco, J. Phys. Chem. B 108 (2004) 5640;
(e) W. Xu, D. Raftery, J. Catal. 204 (2001) 110.

[7] (a) M. Anpo, N. Aikawa, S. Kodama, Y. Kubokawa, J. Phys. Chem. 88 (1984) 3998;
(b) Y. Nosaka, K. Koenuma, K. Ushida, A. Kira, Langmuir 12 (1996) 736;
(c) Y. Nosaka, M. Kishimoto, J. Nishino, J. Phys. Chem. B 102 (1998) 10279.

[8] (a) R. Nakamura, A. Imanishi, K. Murakoshi, Y. Nakato, J. Am. Chem. Soc. 125 (2003) 7443;
(b) G.N. Ekstrom, A.J. Mcquillan, J. Phys. Chem. B 103 (1999) 10562;
(c) S. Sato, K. Ueda, Y. Kawasaki, R.J. Nakamura, J. Phys. Chem. B 106 (2002) 9054;
(d) J.M. Coronada, S. Kataoka, I. Tejedor-Tejedor, M.A. Anderson, J. Catal. 219 (2003) 219;
(e) D.V. Kozlov, E.A. Paukshtis, E.N. Savinov, Appl. Catal. B-Environ. 24 (2000) L7;
(f) W.C. Wu, C. Chuang, J.L. Lin, J. Phys. Chem. B 102 (2000) 8719.

[9] D.S. Muggli, K.H. Lowery, J.L. Falconer, J. Catal. 180 (1998) 111.

[10] (a) G.A. Somorjai, Introduction to Surface Chemistry and Catalysis, John Wiley & Sons, New York, 1994, p. 324;
(b) R.J.H. Clark, R.E. Hester, Spectroscopy for Surface, John Wiley & Sons, New York, 1998, p. 219;
(c) E.P. Parry, J. Catal. 2 (1963) 371;
(d) J.B. Peri, J. Phys. Chem. 69 (1965) 211.

[11] R.M. Alberici, W.F. Jardim, Appl. Catal. B-Environ. 14 (1997) 55.

[12] X.Z. Fu, W.A. Zeltner, Q. Yang, M.A. Anderson, J. Catal. 168 (1997) 428.

[13] J.C. Yu, X.C. Wang, L. Wu, W.K. Ho, L.Z. Zhang, G.T. Zhou, Adv. Funct. Mater. 14 (2004) 1178.

[14] (a) J.R. Sohn, H.J. Jang, M.Y. Park, E.H. Park, S.E.J. Park, Mol. Catal. 93 (1994) 149;
(b) Y. Okamoto, M. Oh-Hara, A. Maezawa, T. Imanaka, S. Teranishi, J. Phys. Chem. 90 (1986) 2396.

[15] T. Yamaguchi, Appl. Catal. 61 (1990) 1.

[16] J.R. Sohn, H.J. Kim, J. Catal. 101 (1986) 428.

[17] (a) O.M. Busch, W. Brijoux, S. Thomson, F. Schuth, J. Catal. 222 (2004) 174;
(b) B.H. Davis, R.A. Keogh, S. Alerasool, D.J. Zalewski, D.E. Day, P.K. Doolin, J. Catal. 183 (1999) 45.

[18] (a) Y. Oosawa, M. Gratzel, J. Chem. Soc. Chem. Commun. (1984) 1629;
(b) M.A. Henderson, W.S. Epling, C.H.F. Peden, C.L. Perkins, J. Phys. Chem. B 107 (2003) 534.

[19] (a) G. Munuera, V. Rives-Arnau, A. Saucedo, J. Chem. Soc. Faraday Trans. 1 75 (1979) 736;
(b) A. Gonzalez-Elipe, G. Munuera, J. Soria, J. Chem. Soc. Faraday Trans. 1 75 (1979) 748;
(c) G. Munuera, A. Gonzalez-Elipe, J. Soria, J. Sanz, J. Chem. Soc. Faraday Trans. 1 76 (1980) 1535;
(d) A. Boonstra, C. Mutsaers, J. Phys. Chem. 79 (1975) 1694;
(e) P. Salvador, C. Gutierrez, Chem. Phys. Lett. 86 (1982) 131;
(f) M. Anpo, K. Chiba, M. Tomonari, S. Coluccia, M. Che, M.A. Fox, Bull. Chem. Soc. Jpn. 64 (1991) 543.

[20] (a) T. Yoshihara, R. Katoh, A. Furube, Y. Tamaki, M. Murai, K. Hara, S. Murata, H. Arakawa, A. Tachiya, J. Phys. Chem. B 108 (2004) 3817;
(b) I.A. Shkrob, M.C. Sauer Jr., J. Phys. Chem. B 108 (2004) 12497;
(c) R. Nakamura, Y. Nakato, J. Am. Chem. Soc. 126 (2004) 1290;
(d) R. Nakamura, T. Tanaka, Y. Nakato, J. Phys. Chem. B 108 (2004) 10617.

[21] (a) C.S. Turchi, D.F. Ollis, J. Catal. 119 (1989) 483;
(b) C.S. Turchi, D.F. Ollis, J. Catal. 122 (1990) 178.

[22] R.B. Draper, M.A. Fox, Langmuir 6 (1990) 1396.

[23] J.M. Warman, M.P. de Haas, P. Pichat, T.P.M. Koster, E.A. van der Zouwen-Assink, A. Mackor, R. Cooper, Radiat. Phys. Chem. 37 (1991) 433.

[24] (a) A. Yamakata, T. Ishibashi, H. Onishi, J. Phys. Chem. B 106 (2002) 9122;
(b) A. Yamakata, T. Ishibashi, H. Onishi, Chem. Phys. Lett. 376 (2003) 576.

[25] O.I. Micic, Y. Zhang, K.R. Cromack, A.D. Trifunac, M.C. Thurnauer, J. Phys. Chem. 97 (1993), 7277/13284.

[26] I.A. Shkrob, M.C. Sauer Jr., D. Gosztola, J. Phys. Chem. B 108 (2004) 12512.

[27] (a) R. Wang, K. Hashimoto, A. Fujishima, M. Chikuni, E. Kojima, A. Kitamura, M. Shimohigoshi, T. Watanabe, Nature 388 (1997) 431;
(b) R. Nakamura, K. Ueda, S. Sato, Langmuir 17 (2001) 2298.
[28] A.Y. Nosaka, E. Kojima, T. Fujiawara, H. Yagi, H. Akutsu, Y. Nosaka, J. Phys. Chem. B 107 (2003) 12042.
[29] X.Z. Fu, L.A. Clark, W.A. Zeltner, M.A. Anderson, J. Photochem. Photobiol. A 97 (1996) 181.
[30] (a) H.K. Park, D.K. Kim, C. Hee, J. Am. Ceram. Soc. 80 (1997) 743;
(b) M. Zheng, M. Gu, Y. Jin, G. Jin, Mater. Sci. Eng. B 77 (2000) 55.
[31] C. Deng, P.F. James, P.V. Wright, J. Mater. Chem. 8 (1998) 153.